Geometries, Electronic *g*-tensor Elements, Hyperfine Coupling Constants, and Vertical Excitation Energies for Small Gallium Arsenide Doublet Radicals, Ga_xAs_y ($x + y = 3, 5$)

Scott Brownridge and Friedrich Grein*

Department of Chemistry, University of New Brunswick, Fredericton, NB, E3B 6E2, Canada

Received: June 5, 2003; In Final Form: August 1, 2003

Geometries of the gallium arsenide doublet radicals $GaAs_2$, Ga_2As, Ga_2As_3, Ga_3As_2, $GaAs_4$, and Ga_4As were optimized by the B3LYP/6-311+G(2df) method and compared with literature values. For the global minimum, as well as for isomers lying up to 0.2 eV higher, hyperfine coupling constants (HFCC) and electron-spin *g*-tensors were calculated. For HFCCs the B3LYP/6-311+G(2df) method was used, whereas for *g*-tensors second-order perturbation calculations with multireference configuration interaction wave functions and a valence triple-ζ basis set with polarization functions (TZVP) were performed. Generally, due to the low s-spin and high p-spin densities, A_{iso} values are small, and A_{dip}'s large. The *g*-shifts ($\Delta g = g - g_e$) are on the order of 100 000 ppm, caused by large spin−orbit couplings and low excitation energies. For the experimentally known Ga_2As_3, values calculated for the D_{3h} structure are (*A*'s in MHz, Δg's in ppm) $A_{iso}(^{69}Ga) = 1325$ (1524); $A_{iso}(^{75}As) = -23$ (65); $A_{dip}(^{69}Ga) = 65$ (87); $A_{dip}(^{75}As) = 36$ (0); $\Delta g_\perp = -73\,410$ (−82 300); and $\Delta g_{||} = 6460$ (0), with magnetic parameters derived from the experimental values in parentheses. Mulliken spin densities are shown to be a good measure of A_{dip} values. Vertical excitation energies, as obtained from the *g*-tensor calculations, are also tabulated.

1. Introduction

To date there have been few experimental electron paramagnetic resonance (EPR) studies on III−V (group 13−group 15 binary compounds) doublet radicals. To our knowledge, such work has been reported only for BNB[1] and Ga_2As_3.[2] For triplet or quartet III−V radicals, experimental EPR data are available for $GaAs^+$ ($X^4\Sigma^-$)[3] and GaP^+ ($X^4\Sigma^-$).[4] For bulk materials, antisite defects (e.g., GaAs−$Al_xGa_{1-x}As$,[5] P_{Ga} in GaP,[6] As_{Ga} in GaAs,[7] and P_{In} in InP[8]) and Ga-vacancies in electron-irradiated GaP[9] have been characterized by EPR spectroscopy.

However there have been many theoretical studies on the electronic states and structures of Ga_xAs_y radicals. Of interest to this work are the neutral doublet radicals $GaAs_2$,[10−15] Ga_2As,[10,12−14] Ga_2As_3,[13,16−18] Ga_3As_2,[13,18] $GaAs_4$, and Ga_4As.[19] Furthermore, calculations on neutral Ga_3As_4,[14,17,20] Ga_4As_3,[14,20] Ga_4As_5,[14,17] and Ga_5As_4[14] and on ionic $Ga_3As^\pm$ and $GaAs_3^\pm$ [21] have been reported. In addition to optimized geometries, Arratia-Pérez and Hernández-Acevedo[16] calculated the *g*-tensor and hyperfine interactions of Ga_2As_3 using the self-consistent Dirac scattered wave method (SCF-DSW-Xα) of Yang et al.[22] and a fully relativistic first-order perturbation procedure, which confirmed Weltner's[2] EPR spectral determination of a trigonal bipyramidal structure for Ga_2As_3. Arratia-Pérez and Hernández-Acevedo have also calculated the *g*-tensors and hyperfine interactions for $GaAs_2$ and Ga_2As.[23]

The focus of this work is the calculation of *g*-tensors and hyperfine coupling constants (HFCC) for all Ga_xAs_y doublet radicals with $x + y = 3$ and 5, namely, $GaAs_2$, Ga_2As, Ga_2As_3, Ga_3As_2, $GaAs_4$, and Ga_4As. Guided by the available literature, new geometry optimizations were performed for various starting structures. In cases of several low-lying isomers, property calculations were performed for all that lie within 0.2 eV of the global minimum.

Due to the scientific and industrial significance of Ga−As semiconductors, as well as the role played by EPR spectroscopy in probing structures and defects,[5−9] the present study is intended to build a base of information, starting with the smallest GaAs radicals and moving to larger ones, eventually including clusters large enough to allow for the modeling of defects. In addition to providing numerical results of use to EPR spectroscopists, we discuss HFCCs and *g*-tensors as to their origin and their relation to other parameters.

2. Methods

Geometry optimizations and HFCC calculations were carried out with the GAUSSIAN 98 suite of programs[24] at the B3LYP/6-311+G(2df) level. Starting structures were those given in the literature, but other possible structures were also examined.

The theoretical evaluation of *g*-tensors using perturbation theory is described in detail in ref 25. The total *g*-shift Δg ($\Delta g = g - g_e$, where $g_e = 2.002319$ is the *g*-factor of a free electron[26]) for a given molecule is comprised of first- and second-order terms. In this paper, only second-order *g*-tensor components were calculated, as the first-order contributions to the total Δg are known to be very small (ca. −100 ppm) in relation to the second-order Δg values. The contribution to Δg (second order) is due to the "magnetic" coupling of an excited state with the ground state (GS) and is proportional to their spin−orbit coupling ($\langle SO \rangle$) and magnetic transition moment ($\langle L \rangle$) matrix elements and inversely proportional to their energy separation (ΔE). The total second-order Δg is calculated as a sum-over-states expansion, which generally involves strong coupling to only the first few low-lying excited states.[27−29]

Computer programs used for *g*-tensor calculations are based on the Turbomole package[30] for efficient integral and SCF

* To whom correspondence should be addressed. Phone: (506) 453-4776. Fax: (506) 453-4981. E-mail: fritz@unb.ca.

10.1021/jp035589d CCC: $25.00
Published on Web 09/10/2003

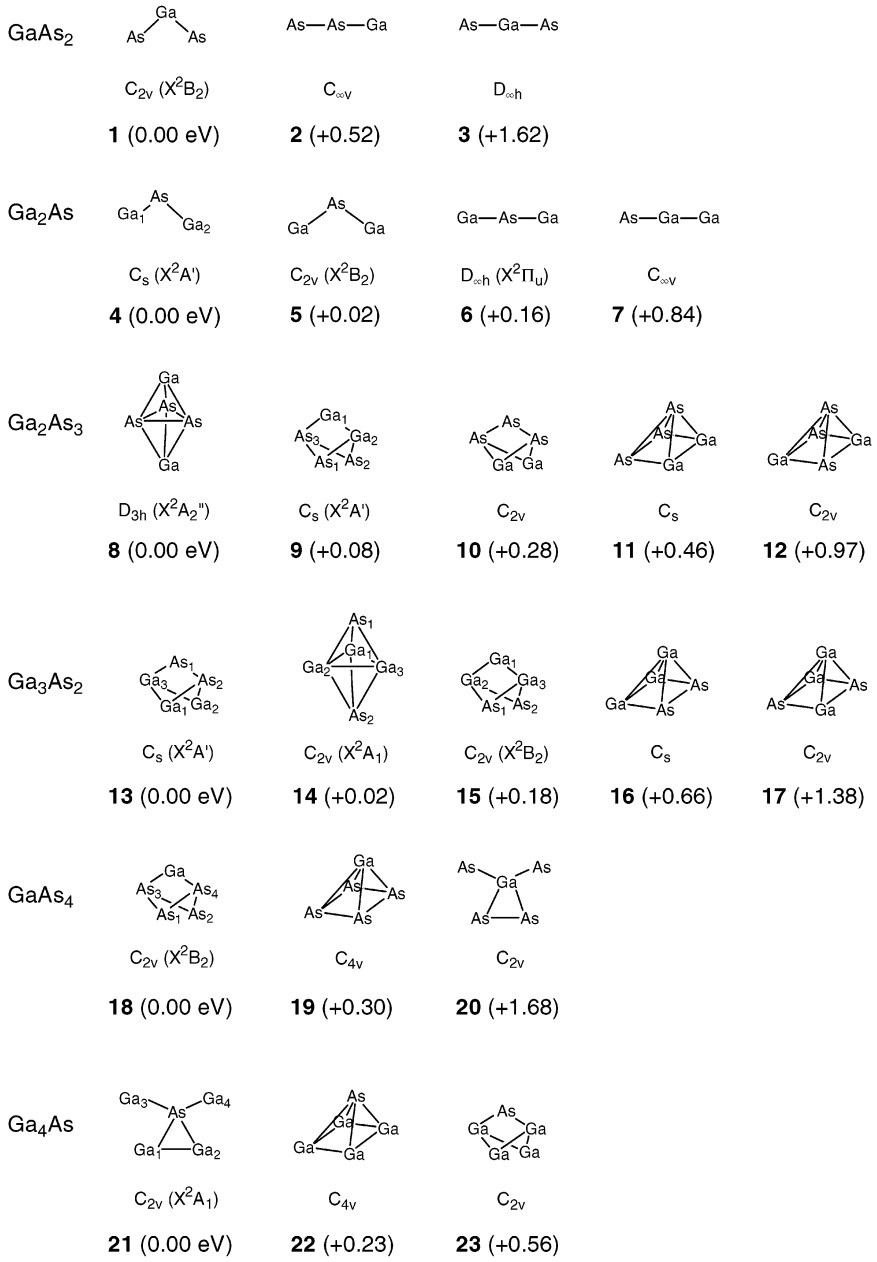

Figure 1. Optimized geometries of Ga_xAs_y ($x + y = 3, 5$) isomers. Bond lengths and angles are given in Table 1.

calculations, on the Grimme−Waletzke multireference configuration interaction (MRCI) package,[31] which also gives the angular momentum matrix elements ($\langle L \rangle$) that we require, and finally on the Marian−Hess mean-field method for calculating spin−orbit integrals[32] as implemented by Schimmelpfennig[33] and adapted for the Grimme MRCI package by Kleinschmidt et al.[34] Here the one- and two-electron spin−orbit elements are calculated from an effective one-electron one-center mean-field approximation. A description of these methods and comparison with results obtained by the original methods can be found in ref 35. The valence triple-ζ basis set with polarization functions (TZVP) by Schäfer et al.[36] was employed in the *g*-tensor calculations. The electronic charge centroid (ECC) is always taken as gauge origin.[37]

3. Results and Discussion

3.1. Optimized Geometries. Geometry optimizations were done at the B3LYP/6-311+G(2df) level of theory. All geometries investigated are shown in Figure 1, which also includes the symmetry group, the state symbol, and the energy difference relative to the most stable form. The results for the lowest-energy structures and for those that lie up to 0.2 eV higher are given in Table 1 and compared with those of previous calculations. For later applications, it should be pointed out that the planar C_{2v} molecules are always placed in the *yz*-plane, but the symmetry plane of C_s molecules is the *xy*-plane.

3.1.1. $GaAs_2$. $GaAs_2$ was first examined in 1987[15] and again in 2000[13] by Balasubramanian as a triangular C_{2v} structure; a 1991 study also considered a linear $C_{\infty v}$ geometry.[12] Work by Meier et al. in 1991[11] examined C_{2v} and linear (D_{4h}, C_{4v}) geometries. In all cases, the ground state was $^2B_2$ in C_{2v} symmetry.

Our results also gave X^2B_2 in C_{2v} symmetry (**1**, see Figure 1) as the lowest-energy state. Alternate possible geometries considered here for $GaAs_2$ were linear $C_{\infty v}$ **2** ($X^2\Pi$, Ga−As−As: Ga−As = 2.48 Å, As−As = 2.16 Å) and $D_{\infty h}$ **3** ($X^2\Pi_g$, As−Ga−As: Ga−As = 2.22 Å) structures that were 0.52 and 1.62 eV, respectively, higher in energy than X^2B_2 (Figure 1).

TABLE 1: Optimized Bond Distances (Å) and Angles (deg) from This Work [B3LYP/6-311+G(2df)] and Comparison to Literature Values for All Ga_xAs_y ($x + y = 3, 5$) Doublet Radicals within 0.2 eV of the Lowest-Energy Structures

molecule[a]	results						
$GaAs_2$ (**1**)	Ga−As	As−As	AsGaAs				
this work	2.775	2.193	46.5				
ref 13	2.800	2.184	45.9				
ref 11	2.86	2.27	46.6				
ref 14	2.73	2.20	47.5				
Ga_2As (**4**)	Ga_1−As	Ga_2−As	Ga−Ga	GaAsGa			
this work	2.305	2.503	3.613	97.3			
ref 13	2.283	2.534	3.41	90.3			
Ga_2As (**5**)	Ga−As	Ga−Ga	GaAsGa				
this work	2.384	3.553	96.3				
ref 13	2.407	3.091	79.9				
ref 14	2.33	3.52	98.0				
Ga_2As_3 (**8**)	Ga−As	As−As	Ga−As−Ga	As−As−As			
this work	2.594	2.555	110.7	60.0			
ref 18	2.589	2.563					
ref 14	2.65	2.62					
Ga_2As_3 (**9**)	Ga_1−Ga_2	As_1−As_2	Ga_1−As_3	Ga_1−As_1	As_1−As_3	As_1−Ga_2	
this work	2.576	2.539	2.523	3.076	2.417	2.639	
		$Ga_2Ga_1As_3$	$Ga_1As_3As_1$	$Ga_1Ga_2As_1$	$Ga_2As_1As_3$		
this work		95.8	77.0	72.3	96.8		
Ga_3As_2 (**13**)	As_1−As_2	Ga_1−Ga_2	As_1−Ga_3	As_1−Ga_1	Ga_1−Ga_3	Ga_1−As_2	
this work	2.361	4.037	2.502	3.008	2.826	2.577	
		$As_2As_1Ga_3$	$As_1Ga_3Ga_1$	$As_1As_2Ga_1$	$As_2Ga_1Ga_3$		
this work		89.7	68.4	74.9	78.7		
Ga_3As_2 (**14**)	Ga_1−Ga_2	Ga_2−Ga_3	Ga_1−As_1	Ga_2−As_1	As_1−As_2		
this work	3.751	3.979	2.446	2.671	2.725		
ref 18	3.702	4.114	2.401	2.725	2.782		
ref 14	3.72	4.57	2.41	2.59	2.70		
		$Ga_2Ga_1Ga_3$	$As_1Ga_1As_2$	$As_1Ga_2As_2$			
this work		64.0	67.7	61.3			
ref 18		67.5	70.8	61.4			
ref 14		70.0	67.9	55.2			
Ga_3As_2 (**15**)	Ga_1−As_1	Ga_1−Ga_2	Ga_2−As_1	As_1−As_2	$Ga_2Ga_1Ga_3$	$Ga_1Ga_2As_1$	$Ga_2As_1Ga_3$
this work	3.202	2.752	2.570	2.452	92.9	73.8	101.8
ref 14	2.65	2.62	2.28	2.24	94.9		
$GaAs_4$ (**18**)[b]	Ga−As_1	Ga−As_3	As_1−As_3	As_1−As_2	As_3GaAs_4	$GaAs_3As_1$	$As_3As_1As_4$
this work	3.116	2.545	2.454	3.006	86.0	77.1	93.4
Ga_4As (**21**)[b]	Ga_1−As	Ga_3−As	Ga_1−Ga_3	Ga_1−Ga_2	Ga_1−Ga_4	Ga_3−Ga_4	
this work	2.588	2.487	2.870	2.599	4.583	4.913	
		Ga_1AsGa_2	Ga_1AsGa_3	Ga_1AsGa_4	Ga_3AsGa_4		
this work		60.3	68.8	129.1	162.0		

[a] See Figure 1 for atom-labeling scheme, symmetry, ground state, and relative energies. [b] No bond lengths or angles given in ref 19.

This compares well to the results of Meier et al.,[11] where X^2B_2 was lower than the $C_{\infty v}$ (Ga−As = 2.61 Å, As−As = 2.24 Å) and $D_{\infty h}$ (2.39 Å) structures by 0.81 and 1.53 eV, respectively.

3.1.2. Ga_2As. For Ga_2As, Balasubramanian reported an X^2B_2 ground state with C_{2v} symmetry (see Table 1) and a C_s (X^2A') structure 0.025 eV higher in energy (multireference singles and doubles configuration interaction (MRSDCI) results).[13] Two low-lying excited states with C_{2v} symmetry, $^2B_1$ (2.52 Å, 108.2°, $\Delta E = +0.22$ eV) and $^2A_1$ (2.47 Å, 118.5°, $\Delta E = +0.19$ eV), were also reported in ref 13.

Our optimized C_{2v} (X^2B_2) geometry (**5**) has a Ga−As−Ga angle of ca. 96° [for the 6-311+G(2df) basis set, B3LYP gave Ga−As 2.384 Å, 96.3°; MPW1PW91 gave 2.358 Å, 93.3°; and MP2 gave 2.365 Å, 103.5°], in close agreement with the local spin-density (LSD) result of 98.0° from ref 14 (see Table 1). However, a slightly lower energy was obtained in C_s symmetry (**4**, X^2A'), 0.02 eV lower than **5**. Our linear $D_{\infty h}$ **6** (2.501 Å, $X^2\Pi_u$) and $C_{\infty v}$ **7** ($X^2\Pi$, As−Ga = 2.286 Å, Ga−Ga = 2.714 Å) were both saddle-point structures, 0.16 and 0.88 eV higher in energy, respectively, than **4**.

3.1.3. Ga_2As_3. The geometry of Ga_2As_3 was predicted in 1992 to be a D_{3h} trigonal bipyramid with an X^2A_2'' ground state, using the LSD method.[14] The EPR spectrum was obtained one year later, from which a trigonal bipyramidal structure was proposed.[2] MRSDCI calculations by Liao et al.[18] and HF followed by MP2 calculations by Piquini et al.[19] also resulted in D_{3h} trigonal bipyramidal structures.

Our calculations showed the lowest-energy structure of Ga_2As_3 to have an X^2A_2'' ground state with D_{3h} trigonal bipyramidal geometry (**8**), in agreement with the structure proposed from the experimental EPR data[2] and previous calculations.[14,18,19]

Alternate possible geometries considered by us, shown in Figure 1, were two edge-capped tetrahedra **9** (C_s, X^2A', +0.08 eV) and **10** (C_{2v}, X^2A_1, +0.28 eV); a C_s square pyramid **11** (X^2A'', +0.46 eV); and a C_{2v} square pyramid **12** (X^2B_1), 0.97 eV higher in energy than **8**.

3.1.4. Ga_3As_2. The lowest-energy Ga_3As_2 isomer reported in refs 14 and 18 was a C_{2v} distorted trigonal bipyramid (X^2A_1, **14** in Figure 1). The isomer **15** (C_{2v} edge-capped tetrahedron, X^2B_1) was reported by Lou et al. to be 0.01 eV higher in energy than **14** (LSD results).[14] Liao et al. found an isomer similar to **15**, but with the Ga_2,Ga_3 (notation according to Figure 1) atoms of **15** switching positions with As_1,As_2, to lie 0.005 eV (MRSDCI; 0.03 eV, CASSCF (complete active space self-consistent field)) above isomer **14**, having a $^2B_1$ ground state.[18]

The distortion from a D_{3h} trigonal bipyramid to C_{2v} symmetry (**14**) was accomplished by having the Ga_1−Ga_2 (and Ga_1−Ga_3)

TABLE 2: Spin Densities (SD), Atomic Charges, and Hyperfine Coupling Constants for ^{69}Ga and ^{75}As (MHz) for All Ga_xAs_y ($x + y = 3, 5$) Doublet Radicals within 0.2 eV of the Lowest-Energy Structures

						calc s- and p-SD[c]	
molecule	atom	charge[a]	spin density[a]	A_{iso}	$T_{xx}/T_{yy}/T_{zz}$[b]	%s	%p
$GaAs_2$ (**1**)	Ga	0.226	0.262	26	−57/131/−74	0.2	32
ref 23		0.193	0.338	52[d]	−85[d]		
	As	−0.113	0.368	7	−111/−113′/225′	<0.1	34
ref 23		−0.096	0.331	229[e]	60[e]		
Ga_2As (**4**)	Ga_1	0.089	0.443	702	227′/−116′/−112	6	55
	Ga_2	0.178	0.048	93	−26′/42′/−16	0.8	10
	As	−0.267	0.508	−133	312′/−155′/−158	0.9	46
Ga_2As (**5**)	Ga	0.128	0.242	447	−63/−81′/144	4	35
ref 23		0.103	0.153	9[f]	−47[f]		
	As	−0.257	0.515	−148	−159/304/−145	1	45
ref 23		−0.206	0.694	124[g]	−56[g]		
Ga_2As_3 (**8**)	Ga	0.194	0.369	1325	−65/−65/129	11	31
expt.[h]				1524	87		
ref 16		0.150	0.314	1583[i]	64[i]		
	As	−0.129	0.088	−23	−35/−36/71	0.2	11
Expt.[h]				64.7[j]	−[j]		
ref 16		−0.100	0.124	88[k]	14[k]		
Ga_2As_3 (**9**)	Ga_1	0.137	0.085	9	−32′/70′/−37	< 0.1	17
	Ga_2	0.147	0.441	1091	−86′/170/−83′	9	42
	As_1, As_2	−0.161	0.068	−4	58′/−33′/−25′	< 0.1	8
	As_3	0.036	0.339	−69	215′/−112′/−104	0.5	32
Ga_3As_2 (**13**)	Ga_1, Ga_2	0.140	0.094	125	−23′/−26′/49′	1	12
	Ga_3	0.195	0.223	19	−62′/123′/−61	0.1	30
	As_1	−0.210	0.338	80	−115′/215′/−100	0.5	32
	As_2	−0.265	0.252	−7	136′/−74′/−62	<0.1	20
Ga_3As_2 (**14**)	Ga_1	0.175	0.426	1735	−85/−71/156	14	38
	Ga_2, Ga_3	0.276	0.085	203	−21/45′/−24′	2	11
	As_1, As_2	−0.363	0.202	−25	−61′/−56/116′	0.2	17
Ga_3As_2 (**15**)	Ga_1	0.276	0.183	−3	−28/81/−53	<0.1	20
	Ga_2,Ga_3	0.098	0.038	−17	−21′/35/−15′	0.1	8
	As_1,As_2	−0.236	0.371	87	−106/−109′/215′	0.6	32
$GaAs_4$ (**18**)	Ga	0.214	−0.038	−153	4/17/−21	1	5
	As_1, As_2	−0.078	0.585	−46	−156/308′/−152′	0.3	46
	As_3, As_4	−0.030	−0.066	12	−10′/45/−36′	0.1	6
Ga_4As (**21**)	Ga_1, Ga_2	0.083	0.342	−122	−89/177′/−88′	1	43
	Ga_3, Ga_4	0.171	0.169	153	−34/−43′/76′	1	19
	As	−0.509	−0.021	0.05	−13/−7/20	<0.1	3

[a] Spin densities and atomic charges from a Mulliken population analysis (this work). [b] T_{xx}', T_{yy}', T_{zz}' are diagonalized values, indicated by a prime after the value. [c] Approximate percent contribution per atom (**X**) to the s- [A_{iso}^{X}(molecule)/A_{iso}^{X}(atom)] and p-character [A_{dip}^{X}(molecule)/A_{dip}^{X}(atom)] of the total SD.[26] [d] Derived from $A_{||}(^{69}Ga) = -118$ MHz, $A_{\perp}(^{69}Ga) = 138$ MHz,[23] using $A_{iso} = 1/3(A_{||} + 2A_{\perp})$ and $A_{dip} = 1/3(A_{||} - A_{\perp})$.[26] [e] Derived from $A_{||}(^{75}As) = 349$ MHz, $A_{\perp}(^{75}As) = 168$ MHz.[23] [f] Derived from $A_{||}(^{69}Ga) = -85$ MHz, $A_{\perp}(^{69}Ga) = 55$ MHz.[23] [g] Derived from $A_{||}(^{75}As) = 11$ MHz, $A_{\perp}(^{75}As) = 180$ MHz.[23] [h] Ref 2, in Ar matrix. $A_{iso}(^{71}Ga) = 1936$ MHz, $A_{dip}(^{71}Ga) = 71$ MHz from EPR spectra for $^{71}Ga_2As_3$ (Ar matrix).[2] From our $A_{iso}(^{69}Ga)$, we obtain $A_{iso}(^{71}Ga) = 1684$ MHz. [i] Derived from $A_{||}(^{69}Ga) = 1711$ MHz, $A_{\perp}(^{69}Ga) = 1519$ MHz.[16] [j] For ^{75}As, it was assumed that $A_{||} - A_{\perp} - A_{iso}$.[2] [k] Derived from $A_{||}(^{75}As) = 116$ MHz, $A_{\perp}(^{75}As) = 75$ MHz.[16]

distance shorter than Ga_2-Ga_3 (see Table 1). Ga_1 lies along the *z*-axis, Ga_2 and Ga_3 along *y*.

Our lowest-energy structure was a C_s edge-capped tetrahedron (**13**), lower than **14** by 0.02 eV. Structure **13** was not mentioned in ref 14, 18, or 19, but simulated annealing results by Vasiliev et al.[38] suggested **13** to be the lowest-energy isomer for Ga_3As_2. Other geometries we investigated were a C_{2v} edge-capped tetrahedron (X^2B_2, **15**) 0.18 eV higher in energy than **13**; a C_s square pyramid (X^2A'', **16**), +0.66 eV; and a C_{2v} square pyramid (X^2A_1, **17**), +1.38 eV.

3.1.5. $GaAs_4$. $GaAs_4$ was included in a study of electronic and structural trends in small GaAs clusters by Piquini et al., who carried out Hartree−Fock optimizations including all electrons and no symmetry constraints, followed by single-point MP2 calculations on the minimum energy configurations.[19] However, they did not report any geometry details other than a sketch of the molecule, the symmetry, and a table of averaged bond orders for only the lowest-energy structure.

Our results gave a C_{2v} edge-capped tetrahedron (X^2B_2, **18** in Figure 1) as the lowest-energy structure, resembling that shown in ref 19. We calculated C_{4v} square pyramidal (X^2A_1, **19**) and C_{2v} planar trapezoidal (X^2B_1, **20**) geometries to be 0.30 and 1.68 eV, respectively, higher in energy than **18**.

3.1.6. Ga_4As. Ga_4As was also included in the study by Piquini et al.,[19] and again no detailed geometrical information was given. The lowest-energy structure we obtained for Ga_4As was a C_{2v} planar trapezoidal structure (X^2A_1) with the As atom in the center (C_{2v}, **21**), similar to Piquini et al.[19] Our results showed square-pyramidal (C_{4v}, X^2B_1, **22**) and C_{2v} edge-capped tetrahedral (X^2A_2, **23**) geometries to be respectively 0.23 and 0.56 eV higher in energy than **21**.

3.2. Hyperfine Coupling Constants. Hyperfine coupling calculations were performed on the lowest-energy structures of each radical, and on structures up to 0.2 eV higher. The atomic charges, Mulliken spin densities (SD), and HFCC data for ^{69}Ga and ^{75}As are given in Table 2. For all the molecules in Table 2, the Ga atoms carry positive charges and the As atoms are negatively charged, as expected since As is more electronegative than Ga.

The Mulliken spin density is the sum of s- and p-spin densities and does not allow for the separation of the two components, which are, in the nonrelativistic treatment, responsible for the

A_{iso} and A_{dip} contributions, respectively. However, since the SOMOs (singly occupied molecular orbitals) are comprised of mainly p orbitals, the s-density in the SOMO, and consequently in the total wave function, is expected to be very small, such that the Mulliken value can be taken as a good measure of the p-density.

Table 2 shows that $A_{iso}(^{69}Ga)$ does not exceed 1735 MHz. Compared to the atomic $A_{iso}(^{69}Ga)$ of 12 210 MHz, as given by Weltner[26] (corresponding to 100% s-density); this indicates a maximal s-density on any of the Ga atoms not exceeding 14% (usually much less). Similarly, the largest positive $A_{iso}(^{75}As)$ is 87 MHz, indicating a very low s-density of 0.6% when compared with the atomic $A_{iso}(^{75}As)$ of 14 660 MHz.[26] Due to such low s-densities, a rationalization of A_{iso} values is quite difficult.

The situation is different for the anisotropic contributions T_{xx}, T_{yy}, and T_{zz}, which are relatively large in comparison with Weltner's atomic values, as is also indicated by the Mulliken spin densities which are essentially of p-type. For example, for Ga_2As_3 (**13**), the Mulliken SDs are 0.094 for Ga_1 and Ga_2, 0.223 for Ga_3, 0.338 for As_1, and 0.252 for As_2. The largest component (the prime stands for diagonalized values) for Ga_1 and Ga_2 is T_{zz}' (49 MHz), and for Ga_3 it is T_{yy}' (123 MHz). Compared to the atomic $A_{dip}[^{69}Ga(4p)] = 408$ MHz,[26] the p_z' spin density for Ga_1 and Ga_2 is 12%, and the p_y' SD for Ga_3 is 30%. Using $A_{dip}[^{75}As(4p)] = 667$ MHz,[26] the p_y' SD for As_1 is 32%, and the p_x' SD for As_2 is 20%. These percentages are roughly proportional to the SD values predicted by the Mulliken analysis (which however lumps all p contributions together).

The s and p spin densities, as derived from the calculated A_{iso} and the largest component of A_{dip}, using the atomic values given by Weltner,[26] are listed in the last two columns of Table 2.

*3.2.1. $GaAs_2$ (**1**).* From our calculated A_{iso} and T_{ii} values in Table 2, the SD (p-type) is equally distributed over each Ga and As atom, with essentially zero s-density. Our Mulliken SDs are in reasonable agreement with the p-SDs obtained for the anisotropic terms. Due to symmetry, the b_2-SOMO has zero s-SD at the Ga atom, and the Hartree−Fock value of A_{iso}(Ga) is exactly zero. The small value actually obtained is due to spin polarization.

Arratia-Pérez et al. calculated $A_{||}$ and $A_{\perp}$ values, assuming $A_{xx} = A_{yy} = A_{\perp}$ and $A_{zz} = A_{||}$ for **1**.[23] From an approximate decomposition of the hyperfine tensors into Fermi, spin-dipolar, and orbital contributions, they estimated the isotropic and anisotropic spin populations. They report for Ga a SD of 0.338 (0.106 isotropic, 0.232 anisotropic) and for As 0.331 (0.121 isotropic, 0.210 anisotropic).

In their relativistic treatment, both $s_{1/2}$ and $p_{1/2}$ atomic spinors contribute to the isotropic component, and therefore a comparison with our nonrelativistic numbers is misleading.

*3.2.2. Ga_2As (**4**, **5**).* According to our calculations, isomers **4** and **5** differ by only 0.02 eV, so it is not clear which isomer will be found experimentally. From the calculated HFCCs, it should be easy to deduce the structure of the eventually observed species, as **4** has an $A_{iso}(^{69}Ga)$ of 702 MHz, whereas that of **5** is 447 MHz. The $A_{iso}(^{75}As)$ values are very similar, and a distinction based them, as well on A_{dip} values, would be difficult.

As with $GaAs_2$ (**1**), the SD of both **4** and **5** is mainly p-type. However, Table 2 shows that A_{iso} for Ga_1 in **4** is much larger than that obtained for **1**, implying the s-density on Ga_1 (6%) to be larger than encountered before. The A_{iso} for each Ga in **5** is also relatively large, with an s-density of about 4%. Also, T_{ii}'s for Ga_1 and As in **4** and As in **5** are larger than values obtained for **1**. In **4**, almost all the SD is on the Ga_1 and As atoms, which comprise the short (2.305 Å) bond; only about 10% p-character is on Ga_2. The calculated p-SDs are in reasonable agreement with the Mulliken SDs.

Our data for **5** correspond to about 35% p-character at each Ga and 45% at the As atom. Arratia-Perez et al. report for Ga a smaller SD of 0.153 (0.057 isotropic, 0.096 anisotropic), and for As a larger SD of 0.694 (0.130 isotropic, 0.564 anisotropic).[23] For **5**, with a $^2B_2$ GS, the SOMO has zero s-SD at the As atom, and therefore (in the nonrelativistic description) A_{iso}(As) is solely due to spin polarization.

*3.2.3. Ga_2As_3 (**8**).* Our calculated $A_{iso}(^{69}Ga) = 1325$ MHz and $A_{dip}(^{69}Ga) = 65$ MHz are in good agreement with the respective magnetic parameters derived from the experimental values of 1524 and 87 MHz.[2] Most of the SD(p) lies on the Ga atoms, in agreement with the Mulliken SD and the SD distribution from ref 16 (see Table 2). In the analysis of the experimental EPR spectra, the assumption was made that for As $A_{||} \cong A_{\perp} \cong A_{iso}$, leading to $A_{iso}(^{75}As) \cong 64.7$ MHz (and implying $A_{dip}(^{75}As) \cong 0$).[2] This has to be contrasted to our ^{75}As result of −23 MHz for A_{iso} and 36 MHz for A_{dip}. The $^2A_2''$ GS does not allow the a_2'' SOMO to have s-orbitals located on the As atoms. Therefore, A_{iso}(As) results solely from spin polarization and is negative, as was proposed earlier by Van Zee, Li, and Weltner.[2]

*3.2.4. Ga_2As_3 (**9**).* This isomer lies, according to our calculations, 0.08 eV above structure **8**. The A_{iso} and T_{ii} values calculated for this isomer differ strongly from that of **8** and confirm the latter to be the experimental structure. The majority of the SD in **9** is on Ga_2 (p_y, ca. 42%) and As_3 (p_x', ca. 32%), with respective Mulliken SDs of 0.441 and 0.339.

*3.2.5. Ga_3As_2 (**13**, **14**, **15**).* For Ga_3As_2, three structures lie within 0.2 eV, with **13** the lowest, **14** calculated to be 0.02 eV higher, and **15** 0.18 eV higher. Therefore **13** and **14** are contenders for the equilibrium form of Ga_3As_2 and should be distinguishable by their HFCC values. For **13**, the largest A_{iso} is 125 MHz (on Ga_1, Ga_2), and for **14** it is 1735 MHz (on Ga_1), about 14 times larger. The largest A_{iso} of **15** is 87 MHz (on As_1, As_2), with anisotropic components up to 215 MHz.

*3.2.6. $GaAs_4$ (**18**).* For $GaAs_4$ (**18**) in C_{2v} symmetry, all A_{iso}'s are small (implying little s-density), whereas the components of A_{dip} for As_1 and As_2 are relatively large. Accordingly, the majority of SD lies on As_1 and As_2 (46%), with very little contribution from the other three atoms, in good agreement with the Mulliken values.

*3.2.7. Ga_4As (**21**).* Again, A_{iso} is small, and for the Ga atoms A_{iso} and A_{dip} values are of similar magnitude. Most of the Mulliken SD resides on Ga_1 and Ga_2 (0.342), as reflected in the large A_{dip} component of these atoms. The very small Mulliken SD on As (−0.021) agrees with small $A_{dip}(^{75}As)$ values, corresponding to a maximal p-density of about 3%.

3.3. *g*-Tensors. For molecules with C_{2v} symmetry, the three components of Δg (in the order *x*, *y*, *z*) arise from coupling with $^2B_2$, $^2B_1$, and $^2A_2$ excited states if the GS is $^2A_1$ (**14**, **21**), from coupling with $^2A_2$, $^2A_1$, and $^2B_2$ states if the GS is $^2B_1$ (**8**, from X^2A_2'' in D_{3h}), and from coupling with $^2A_1$, $^2A_2$, and $^2B_1$ states if the GS is $^2B_2$ (**1**, **5**, **15**, **18**). For molecules with C_s symmetry and X^2A' (**4**, **9**, **13**), Δg_{xx} and Δg_{yy} result from coupling with $^2A''$ states, and Δg_{zz} from coupling with $^2A'$ states. With the atoms placed in the *xy*-plane, the *x* and *y* components of Δg mix, and a matrix diagonalization is required.

Table 3 summarizes our total Δg (second-order) values and compares them to known experimental and theoretical results. Experimental *g*-tensor results are available only for Ga_2As_3,[2]

TABLE 3: Calculated *g*-Tensor Data (Δg in ppm) for Ga_xAs_y ($x + y = 3, 5$) and Comparison with Experimental and Other Theoretical Results

molecule	Δg_{xx}	Δg_{yy}	Δg_{zz}	$\langle\Delta g\rangle^c$
$GaAs_2$ (**1**)	175 300	−175 120	−18 280	−6035
ref 23, calc[a]	95 600	95 600	−116 500	24 900
Ga_2As (**4**)	28 370	−11 285	−78 000	−20 305
Ga_2As (**5**)	−125 950	−24 850	51 030	−33 260
ref 23, calc[a]	−188 500	−188 500	40 100	−112 300
Ga_2As_3 (**8**)	−73 410[b]	−73 410[b]	6460	−46 790
ref 2, expt	−82 300	−82 300	−0	−54 870
ref 16, calc	−148 000	−148000	−162 00	−104 070
Ga_2As_3 (**9**)	−63 625	−3540	−101 270	−56 145
Ga_3As_2 (**13**)	135 055	−15 070	104 970	74 985
Ga_3As_2 (**14**)	−71 590	−11 150	13 270	−23 155
Ga_3As_2 (**15**)	180 375	257 660	58 025	165 355
$GaAs_4$ (**18**)	−171 030	−7540	−14 720	−64 430
Ga_4As (**21**)	−123 540	−21 850	−43 470	−62 955

[a] Ref 23 reports values for $\Delta g_{\parallel} = \Delta g_{zz}$ and $\Delta g_{\perp} = \Delta g_{xx} = \Delta g_{yy}$. [b] Average of Δg_{xx} and Δg_{yy} from C_{2v} symmetry. [c] Average of the three Δg components.

whereas theoretical results have been reported for Ga_2As_3,[16] $GaAs_2$, and Ga_2As.[23]

Initially, nine excited states were calculated for each irreducible representation and used in the sum-over-states expansion. However, when significant magnetic coupling with the ground state (large $\langle SO\rangle$, $\langle L\rangle$) was still observed in the higher states, the number of excited states was increased. This will be outlined in the individual cases.

For an analysis of the *g*-tensor results, in Table 4 ΔE, $\langle SO\rangle$, $\langle L\rangle$, and Δg values are given for the two excited states having the strongest magnetic coupling with the ground state, for each irreducible representation. In Supporting Information tables, such information is extended to include the first five excited states and those additional states having a large magnetic coupling (>1000 ppm) with the ground state.

Table 3 shows that most $|\Delta g|$ values are on the order of 100 000 ppm. Such large numbers are mainly due to the large spin−orbit matrix elements for Ga and As. The atomic spin−orbit constants are 464 cm^{-1} for Ga and 1201 cm^{-1} for As.[39] Molecular SO coupling constants are on the order of 200−300 cm^{-1}. Combining in the second-order perturbation expression ($\langle SO\rangle\langle L\rangle/\Delta E$), $\langle SO\rangle = 200$ cm^{-1} with $\langle L\rangle = 1$ au and $\Delta E = 1$ eV, leads to a Δg contribution of about (±) 100 000 ppm, changing the free electron g_e of 2.002319 by (±) 0.1.

3.3.1. $GaAs_2$ (1). It is seen that Δg_{xx} and Δg_{yy} are both large, of similar magnitude but opposite sign, whereas Δg_{zz} only has about a tenth of that magnitude. Table 4 shows that Δg_{xx} for $GaAs_2$ is governed by the coupling of 1^2A_1 ($4a_1 \rightarrow 2b_2$, SOMO−1 to SOMO) and 2^2A_1 ($3a_1 \rightarrow 2b_2$, SOMO−3 to

TABLE 4: Calculated Values of ΔE, $\langle SO\rangle$, $\langle L\rangle$, and Δg (second order) for Two Excited States of Each Irreducible Representation Having the Largest Magnetic Couplings with the Ground State for Ga_xAs_y ($x + y = 3, 5$), Given in the Order Δg_{xx}, Δg_{yy}, Δg_{zz}

state	ΔE (eV)	$\langle SO\rangle$ (cm^{-1})	$\langle L\rangle$ (au)	Δg (ppm)	state	ΔE (eV)	$\langle SO\rangle$ (cm^{-1})	$\langle L\rangle$ (au)	Δg (ppm)
$GaAs_2$ (1)									
1^2A_1	1.47	170	1.10	64 366	2^2A_1	2.67	475	1.11	99 952
1^2A_2	1.26	476	−0.90	−172 824	3^2A_2	3.90	−86	1.53	−17 199
5^2B_1	3.61	348	0.98	48 315	6^2B_1	3.89	191	−1.61	−40 264
Ga_2As (4)[a]									
$1^2A''$	0.40	−156	−0.21	42 478	$7^2A''$	3.27	−147	0.57	−13 133
$1^2A''$	0.40	192	0.14	33 996	$7^2A''$	3.27	236	−1.09	−40 168
$3^2A'$	2.06	198	−0.67	−32 718	$5^2A'$	2.66	220	−0.89	−37 334
Ga_2As (5)									
1^2A_1	0.17	177	−0.07	−36 004	2^2A_1	1.97	243	−1.02	−64 115
2^2A_2	2.57	157	−0.48	−14 834	4^2A_2	3.32	159	−0.78	−19 071
1^2B_1	0.33	255	0.22	87 664	5^2B_1	3.32	−220	1.07	−35 932
Ga_2As_3 (8)									
3^2A_1	3.30	343	−1.78	−94 074	5^2A_1	3.70	247	0.63	21 549
2^2B_2	3.28	−356	1.76	−97 100	4^2B_2	3.67	269	0.71	26 635
3^2A_2	2.89	72	0.40	5083	6^2A_2	4.09	195	0.08	2041
Ga_2As_3 (9)[a]									
$5^2A''$	3.02	181	−0.68	−20 852	$7^2A''$	3.71	111	−0.74	−11 141
$2^2A''$	2.67	41	−0.63	−4922	$5^2A''$	3.02	−297	0.52	−26 129
$2^2A'$	1.95	230	−1.09	−65 848	$4^2A'$	2.56	274	−0.59	−32 219
Ga_3As_2 (13)[a]									
$1^2A''$	0.62	228	0.83	155 983	$3^2A''$	1.91	−148	0.88	−34 778
$1^2A''$	0.62	158	0.10	12 691	$3^2A''$	1.91	−183	0.60	−29 048
$2^2A'$	1.44	148	0.76	40 103	$4^2A'$	2.22	308	0.78	54 851
Ga_3As_2 (14)									
1^2B_2	0.72	−72	0.53	−26 906	3^2B_2	2.94	221	−1.40	−53 718
1^2B_1	1.15	80	0.90	32 076	3^2B_1	2.94	321	−0.60	−33 328
1^2A_2	1.00	77	0.39	15 339	3^2A_2	2.79	75	−1.12	−15 409
Ga_3As_2 (15)									
1^2A_1	1.21	202	0.99	83 378	2^2A_1	1.97	370	0.97	93 261
1^2A_2	0.74	383	0.97	256 975	11^2A_2	4.22	−68	1.16	−9479
1^2B_1	0.92	127	0.86	60 313	10^2B_1	4.26	−117	0.70	−9812
$GaAs_4$ (18)									
1^2A_1	0.55	390	−0.50	−179 018	2^2A_1	2.22	−249	1.05	−59 761
1^2A_2	1.91	−312	0.81	−66 989	2^2A_2	2.32	162	1.38	49 104
1^2B_1	1.90	286	0.78	59 501	2^2B_1	2.57	−260	1.29	−66 074
Ga_4As (21)									
1^2B_2	1.28	223	−1.22	−108 538	2^2B_2	1.59	−52	1.40	−23 187
6^2B_1	2.92	−31	1.61	−8668	7^2B_1	3.06	−72	0.72	−8675
6^2A_2	3.44	216	−0.42	−13 477	7^2A_2	3.26	206	−0.45	−14 511

[a] Undiagonalized Δg_{xx} and Δg_{yy} (C_s symmetry).

SOMO) with X^2B_2, both contributing positively, as expected for DOMO (doubly occupied molecular orbital) → SOMO contributions.

The Δg_{yy} component is dominated by the coupling with 1^2A_2 ($2b_2 \rightarrow 2b_1$, SOMO to LUMO+1). Following the rules for SOMO → LUMO (lowest unoccupied molecular orbital) excitations, this term is negative. Since the GS of $GaAs_2$ has no occupied a_2-orbital, DOMO → SOMO type single excitations (with positive Δg) are not possible. Strong couplings with the three-open-shell states 2^2A_2 and 3^2A_2 almost cancel each other: their individual Δg_{yy} contributions are similar in magnitude but opposite in sign (due to the ⟨L⟩'s having opposite sign). This is a general trend observed for a pair of states generated by the same three-open-shell configuration.[27,40,41] In the case of $GaAs_2$, the ΔE and ⟨SO⟩ values for 2^2A_2 and 3^2A_2 are similar, but the ⟨L⟩ values differ by ca. 50% (and have opposite sign). This variation of the ⟨L⟩ values occurs since although the leading configuration for both 2^2A_2 and 3^2A_2 is a $4a_1 \rightarrow 2b_1$ excitation (90% and 85%, respectively), there are differences in the other configurations contributing to 2^2A_2 and 3^2A_2.

For the total Δg_{zz} component the strongest couplings with X^2B_2 arise from 5^2B_1 and 6^2B_1, but their Δg contributions almost cancel each other, since both of these states derive from the same three-open-shell configuration ($3a_1 \rightarrow 1a_2$, SOMO−3 to LUMO). The ΔE's for the two states are very close, but the larger ⟨SO⟩ value of 5^2B_1 is compensated by 6^2B_1 having a larger ⟨L⟩ (in magnitude).

Arratia-Pérez et al.[23] calculated *g*-shifts for $GaAs_2$ utilizing a fully relativistic first-order perturbation procedure based on the SCF-DSW-Xα method.[22] These authors assumed $\Delta g_{xx} = \Delta g_{yy} = \Delta g_{\perp}$ and $\Delta g_{zz} = \Delta g_{||}$ (see also section 3.2.1). As Table 3 shows, our results differ from theirs, both in magnitude (factor of 2−6) and sign (Δg_{yy}). There are no experimental EPR data available for $GaAs_2$ to gauge the accuracy of either result.

3.3.2. Ga_2As (4). For Ga_2As with structure **4** (C_s symmetry), Δg_{xx} and Δg_{yy} are relatively small, whereas Δg_{zz} is in the 100 000 ppm range. Twenty roots were calculated, since significant magnetic coupling was observed in the higher $^2A'$ and $^2A''$ states of an initial 9-root calculation.

The undiagonalized Δg_{xx} is dominated by coupling to $1^2A''$ ($1a'' \rightarrow 5a'$, SOMO−2 → SOMO), giving, as expected, a positive contribution. However, significant (>1000 ppm) negative contributions arise from coupling with a number of other states ($7^2A''$ given in Table 4, others given in Table 2S of the Supporting Information), lowering the total Δg_{xx} (undiagonalized) to 23 280 ppm.

The undiagonalized *yy* component is composed of a number of states contributing positively and negatively in an almost equal manner, resulting in a small overall total for 20 roots.

The Δg_{zz} value is dominated by large negative contributions from $3^2A'$ ($4a' \rightarrow 6a'$, SOMO−1 → LUMO) and $5^2A'$ ($5a' \rightarrow 6a'$, SOMO → LUMO), which constitute 90% of the total Δg_{zz}. Smaller but important (>1000 ppm) positive and negative contributions arise from coupling with a number of other states (values given in Table 2S), adding −8000 ppm to the undiagonalized Δg_{zz}.

3.3.3. Ga_2As (5). Structure **5** of Ga_2As lies 0.02 eV above structure **4**, discussed before. It is a possible contender for the equilibrium structure. Contrary to the *g*-tensor results for **4**, **5** has a large Δg_{xx}, whereas Δg_{yy} and Δg_{zz} differ by a factor of 1.5−2 (in magnitude) from those of structure **4**.

The Δg_{xx} value of Ga_2As (**5**) is dominated by coupling with four states, $1^2A_1-4^2A_1$, all making large negative contributions to Δg_{xx}, countered to a small extent by 6^2A_1 (only 1^2A_1 and 2^2A_1 are given in Table 4). The 1^2A_1 state has a very low excitation energy of 0.17 eV, whose strong contribution to Δg is countered by a small ⟨L⟩ value (−0.07 au). Contrary to expectations, this excited state, of DOMO → SOMO type, makes a negative contribution to Δg (the rule may not apply if $|\langle L\rangle|$ is small).

The two largest contributions to Δg_{yy} are negative values from 2^2A_2 and 4^2A_2, countered by a positive one from 5^2A_2. As the leading configurations for 4^2A_2 and 5^2A_2 are the same ($3a_1 \rightarrow 2b_1$), the ΔE and $|\langle L\rangle|$ values are similar, but the ⟨SO⟩ values differ by ca. 50%. This is due to 4^2A_2 having more mixing with additional configurations, in particular with a double excitation from the SOMO−1 to the SOMO and LUMO+1 ($3a_1^2 \rightarrow 2b_2$-$1a_2$). As there are no occupied a_2-orbitals in the GS, singly excited $^2A_2$ states can be obtained only by SOMO → LUMO type excitations, giving negative Δg's.

The Δg_{zz} value is dominated by coupling to 1^2B_1, with a positive contribution due to its DOMO → SOMO ($1b_1 \rightarrow 2b_2$) excitation. There are smaller contributions from $3,5,6^2B_1$. The 5^2B_1 and 6^2B_1 states have the same leading three-open-shell configuration, SOMO−1 ($3a_1$) to the LUMO+2 ($1a_2$), but again the Δg contributions from these two states do not cancel due to differences in the configuration setup.

As with $GaAs_2$, only $\Delta g_{||}$ and $\Delta g_{\perp}$ values for Ga_2As (**5**) are given in ref 23. Their results for $\Delta g_{\perp} = \Delta g_{xx} = \Delta g_{yy}$ are significantly different from our Δg_{xx} and Δg_{yy} values (by factors of 1.5−7.5), but their Δg_{zz} (= $\Delta g_{||}$) value is in reasonable agreement with ours.

Comparing the Ga_2As structures **4** and **5**, the out-of-plane components (Δg_{xx} of **5**, Δg_{zz} of **4**) differ by about 50 000 ppm, whereas the Ga−Ga components (Δg_{yy} of **5**, Δg_{xx} of **4**) are of similar magnitude but opposite in sign. On the basis of these results, and the ones given in the hyperfine section, an easy distinction between the two isomers should be possible.

*3.3.4. Ga_2As_3 (**8**).* This molecule has D_{3h} symmetry (X^2A_2''), but our Δg calculations were done in the Abelian group C_{2v} (X^2B_1). In this case, the $^2A_1$ and $^2B_2$ states correspond to $^2E'$. For checking the accuracy of our calculations, we calculated Δg for both $^2A_1$ and $^2B_2$ states. Due to the independent selection of reference configurations and extrapolation for $^2A_1$ and $^2B_2$ states, slightly different values were obtained for Δg_{xx} and Δg_{yy}, and the average will be given. Table 4 and the Supporting Information tables list results for Δg_{xx} and Δg_{yy} separately.

For Ga_2As_3, experimental *g*-tensor results are available.[2] The degenerate component agrees within 10% with our result, whereas the parallel component (Δg_{zz}) could not be measured and was assumed to be ≅0 ppm in the experiment, but calculated to be 6460 ppm. It is seen from Table 3 that theoretical literature values, ref 16, differ widely from our and the experimental results.

The values of Δg_{xx} and Δg_{yy} are dominated by coupling of the ground state with 3^2A_1 and 2^2B_2, respectively, corresponding to excitation from the SOMO ($3b_1$) to the degenerate LUMO ($6a_1$) for Δg_{xx} and LUMO+1 ($3b_2$) for Δg_{yy} (negative contributions, as expected). The second largest contribution is from 5^2A_1, an excitation from the SOMO to the degenerate LUMO+4 ($7a_1$), and from 4^2B_2, SOMO to LUMO+3 ($5b_2$) (positive contribution). The remaining major excited-state couplings involve $6,7^2A_1$ and $5,6^2B_2$, excitations from the degenerate SOMO−2 ($1a_2$, Δg_{xx}) and SOMO−1 ($2b_1$, Δg_{yy}) to the LUMO+2 ($4b_2$), resulting in three-open-shell configurations. The ΔE and ⟨SO⟩ values for 5^2B_2 and 6^2B_2 are very similar, but the ⟨L⟩'s have opposite sign, as reflected in their Δg contribution.

TABLE 5: Vertical Excitation Energies (eV) and Leading Configurations for the First Five States of Ga_xAs_y ($x + y = 3, 5$)

state	1	2	3	4	5
$GaAs_2$ (1)			...$1b_2^2 1b_1^2 4a_1^2 2b_2^1$ (13 VE)[a]		
$^2A_1$	1.47 ($4a_1 \rightarrow 2b_2$)	2.67 ($3a_1 \rightarrow 2b_2$)	2.89 ($1b_1 \rightarrow 1a_2$)	3.97 ($2b_2 \rightarrow 5a_1$)	4.24 ($1b_1 \rightarrow 1a_2$)
$^2A_2$	1.26 ($2b_2 \rightarrow 1a_2$)	3.19 ($4a_1 \rightarrow 2b_1$)	3.90 ($4a_1 \rightarrow 2b_1$)	4.37 ($3a_1 4a_1 \rightarrow 2b_2 1a_2$)	4.71 ($4a_1^2 \rightarrow 2b_2 1a_2$)
$^2B_1$	2.27 ($2b_2 \rightarrow 2b_1$)	2.55 ($1b_1 \rightarrow 2b_2$)	2.62 ($4a_1 \rightarrow 1a_2$)	3.13 ($4a_1 \rightarrow 1a_2$)	3.61 ($3a_1 \rightarrow 1a_2$)
$^2B_2$	0.00 (GS)	3.58 ($2b_2 \rightarrow 3b_2$)	4.25 ($1b_1 4a_1 \rightarrow 2b_2 1a_2$)	4.35 ($4a_1 2b_2 \rightarrow 1a_2 2b_1$)	4.76 ($1b_1 \rightarrow 2b_1$)
Ga_2As (4)			...$1a''^2 4a'^2 5a'^1$(11 VE)		
$^2A'$	0.00 (GS)	0.40 ($4a' \rightarrow 5a'$)	2.06 ($4a' \rightarrow 6a'$)	2.30 ($4a' \rightarrow 6a'$)	2.66 ($5a' \rightarrow 6a'$)
$^2A''$	0.40 ($1a'' \rightarrow 5a'$)	2.43 ($1a'' \rightarrow 6a'$)	2.57 ($4a' \rightarrow 2a''$)	2.62 ($1a'' \rightarrow 6a'$)	2.90 ($1a''4a' \rightarrow 5a'6a'$)
Ga_2As (5)			...$1b_2^2 1b_1^2 3a_1^2 2b_2^1$ (11 VE)		
$^2A_1$	0.17 ($3a_1 \rightarrow 2b_2$)	1.97 ($2b_2 \rightarrow 4a_1$)	2.72 ($1b_1 \rightarrow 1a_2$)	2.90 ($3a_1^2 \rightarrow 2b_2 4a_1$)	3.38 ($1b_1 \rightarrow 1a_2$)
$^2A_2$	2.32 ($1b_1 \rightarrow 4a_1$)	2.57 ($2b_2 \rightarrow 1a_2$)	2.78 ($1b_1 \rightarrow 4a_1$)	3.32 ($3a_1 \rightarrow 2b_1$)	3.82 ($3a_1 \rightarrow 2b_1$)
$^2B_1$	0.33 ($1b_1 \rightarrow 2b_2$)	2.57 ($1b_1 3a_1 \rightarrow 2b_2 4a_1$)	2.66 ($3a_1 \rightarrow 1a_2$)	3.01 ($1b_1 3a_1 \rightarrow 2b_2 4a_1$)	3.32 ($3a_1 \rightarrow 1a_2$)
$^2B_2$	0.00 (GS)	2.24 ($3a_1 \rightarrow 4a_1$)	2.65 ($3a_1 \rightarrow 4a_1$)	3.17 ($1b_1 3a_1 \rightarrow 2b_2 1a_2$)	3.41 ($2b_2 \rightarrow 3b_2$)
Ga_2As_3 (8)			...$2b_2^2 5a_1^2 1a_2^2 2b_1^2 3b_1^1$ (21 VE)		
$^2A_1$	1.98 ($5a_1 63b_1$)	2.98 ($4a_1 \rightarrow 3b_1$)	3.30 ($3b_1 \rightarrow 6a_1$)	3.87 ($3a_1 \rightarrow 3b_1$)	3.70 ($3b_1 \rightarrow 7a_1$)
$^2A_2$	1.58 ($1a_2 \rightarrow 3b_1$)	3.64 ($5a_1 \rightarrow 4b_2$)	2.89 ($4a_1 \rightarrow 4b_2$)	4.55 ($3b_1 \rightarrow 2a_2$)	3.85 ($5a_1 \rightarrow 4b_2$)
$^2B_1$	0.00 (GS)	1.58 ($2b_1 \rightarrow 3b_1$)	3.85 ($2b_2 \rightarrow 4b_2$)	4.54 ($3b_1 \rightarrow 4b_1$)	4.50 ($2b_2 \rightarrow 4b_2$)
$^2B_2$	2.69 ($2b_2 \rightarrow 3b_1$)	3.28 ($3b_1 \rightarrow 3b_2$)	3.50 ($3b_1 \rightarrow 4b_2$)	3.67 ($3b_1 \rightarrow 5b_2$)	3.83 ($2b_1 \rightarrow 4b_2$)
Ga_2As_3 (9)			...$7a'^2 3a''^2 8a'^1$ (21VE)		
$^2A'$	0.00 (GS)	1.95 ($8a' \rightarrow 9a'$)	2.25 ($7a' \rightarrow 8a'$)	2.56 ($6a' \rightarrow 8a'$)	3.38 ($3a'' \rightarrow 5a''$)
$^2A''$	1.36 ($3a'' \rightarrow 8a'$)	2.67 ($3a'' \rightarrow 9a'$)	3.07 ($3a'' \rightarrow 9a'$)	2.85 ($2a'' \rightarrow 8a'$)	3.02 ($8a' \rightarrow 4a''$)
Ga_3As_2 (13)	...$6a'^2 3a''^2 7a'^1$ (19 VE)				
$^2A'$	0.00 (GS)	1.44 ($6a' \rightarrow 7a'$)	1.77 ($7a' \rightarrow 8a'$)	2.22 ($5a' \rightarrow 7a'$)	2.57 ($3a'' \rightarrow 4a''$)
$^2A''$	0.62 ($3a'' \rightarrow 7a'$)	1.15 ($2a'' \rightarrow 7a'$)	1.91 ($7a' \rightarrow 4a''$)	2.31 ($3a'' \rightarrow 8a'$)	2.56 ($3a'' \rightarrow 8a'$)
Ga_3As_2 (14)			...$4a_1^2 2b_1^2 1a_2^2 2b_2^2 5a_1^1$ (19 VE)		
$^2A_1$	0.00 (GS)	1.68 ($4a_1 \rightarrow 5a_1$)	2.18 ($2b_2 \rightarrow 3b_2$)	2.56 ($2b_1 \rightarrow 3b_1$)	2.90 ($2b_2 \rightarrow 3b_2$)
$^2A_2$	1.00 ($1a_2 \rightarrow 5a_1$)	2.73 ($2b_2 \rightarrow 3b_1$)	2.79 ($2b_2 \rightarrow 3b_1$)	3.05 ($1a_2 \rightarrow 6a_1$)	2.92 ($1a_2 \rightarrow 6a_1$)
$^2B_1$	1.15 ($2b_1 \rightarrow 5a_1$)	2.52 ($1a_2 \rightarrow 3b_2$)	2.94 ($5a_1 \rightarrow 3b_1$)	2.58 ($1a_2 \rightarrow 3b_2$)	3.90 ($2b_1 \rightarrow 6a_1$)
$^2B_2$	0.72 ($2b_2 \rightarrow 5a_1$)	1.87 ($1a_2 \rightarrow 3b_1$)	2.94 ($5a_1 \rightarrow 3b_2$)	2.52 ($1a_1 \rightarrow 3b_1$)	2.94 ($2b_2 \rightarrow 6a_1$)
Ga_3As_2 (15)			..$5a_1^2 2b_1^2 1a_2^2 1b_2^2 2b_2^1$ (19 VE)		
$^2A_1$	1.21 ($5a_1 \rightarrow 2b_2$)	1.97 ($4a_1 \rightarrow 2b_2$)	2.15 ($1a_2 \rightarrow 3b_1$)	2.44 ($1a_2 \rightarrow 3b_1$)	2.48 ($3a_1 \rightarrow 2b_2$)
$^2A_2$	0.74 ($1a_2 \rightarrow 2b_2$)	2.42 ($5a_1 \rightarrow 3b_1$)	2.90 ($1a_2 2b_1 \rightarrow 2b_2 3b_1$)	2.96 ($5a_1 \rightarrow 3b_1$)	3.17 ($2b_1 \rightarrow 6a_1$)
$^2B_1$	0.92 ($2b_1 \rightarrow 2b_2$)	1.96 ($2b_2 \rightarrow 3b_1$)	3.06 ($2b_1^2 \rightarrow 2b_2 3b_1$)	3.28 ($1a_2 \rightarrow 6a_1$)	3.51 ($1a_2 \rightarrow 6a_1$)
$^2B_2$	0.00 (GS)	1.98 ($2b_1 \rightarrow 3b_1$)	2.47 ($2b_1 \rightarrow 3b_1$)	3.13 ($2b_2 \rightarrow 3b_2$)	3.28 ($5a_1 1a_2 \rightarrow 2b_2 3b_1$)
$GaAs_4$ (18)			...$1a_2^2 2b_2^2 3b_1^2 5a_1^2 3b_2^1$ (23 VE)		
$^2A_1$	0.55 ($3b_2 \rightarrow 6a_1$)	2.22 ($5a_1 \rightarrow 3b_2$)	2.46 ($3b_2 \rightarrow 7a_1$)	2.82 ($2b_2 \rightarrow 6a_1$)	2.61 ($2b_2 \rightarrow 6a_1$)
$^2A_2$	1.91 ($3b_1 \rightarrow 6a_1$)	2.32 ($3b_1 \rightarrow 6a_1$)	3.06 ($3b_2 \rightarrow 2a_2$)	3.37 ($2b_1 \rightarrow 6a_1$)	3.18 ($2b_1 \rightarrow 6a_1$)
$^2B_1$	1.90 ($3b_1 \rightarrow 3b_2$)	2.57 ($3b_2 \rightarrow 4b_1$)	2.40 ($3b_1 3b_2 \rightarrow 6a_1^2$)	3.10 ($2b_1 \rightarrow 3b_2$)	3.19 ($3b_1 \rightarrow 4b_2$)
$^2B_2$	0.00 (GS)	1.62 ($3b_2 \rightarrow 4b_2$)	2.60 ($5a_1 \rightarrow 6a_1$)	2.54 ($2b_2 \rightarrow 3b_2$)	2.63 ($2b_2 63b_2$)
Ga_4As (21)			...$1b_1^2 4a_1^2 3b_2^2 5a_1^1$ (17 VE)		
$^2A_1$	0.00 (GS)	1.66 ($4a_1 \rightarrow 5a_1$)	2.79 ($3b_2 \rightarrow 4b_2$)	2.80 ($3b_2 \rightarrow 4b_2$)	3.02 ($1b_1 \rightarrow 2b_1$)
$^2A_2$	1.22 ($5a_1 \rightarrow 1a_2$)	2.49 ($4a_1 \rightarrow 1a_2$)	2.62 ($4a_1 \rightarrow 1a_2$)	2.42 ($3b_2 \rightarrow 2b_1$)	2.93 ($1b_1 \rightarrow 4b_2$)
$^2B_1$	1.45 ($5a_1 \rightarrow 2b_1$)	2.23 ($1b_1 \rightarrow 5a_1$)	2.03 ($3b_2 \rightarrow 1a_2$)	2.44 ($3b_2 \rightarrow 1a_2$)	2.75 ($4a_1 \rightarrow 2b_1$)
$^2B_2$	1.28 ($5a_1 \rightarrow 4b_2$)	1.59 ($3b_2 \rightarrow 5a_1$)	2.73 ($2b_2 \rightarrow 5a_1$)	2.98 ($1b_1 \rightarrow 1a_2$)	3.02 ($1b_1 \rightarrow 1a_2$)

[a] VE = valence electrons.

The Δg_{zz} was calculated to be an order of magnitude smaller than Δg_{xx} and Δg_{yy}, with the largest contribution from coupling with the 3^2A_2 state, an excitation from SOMO−5 ($4a_1$) to LUMO+2 ($4b_2$). In D_{3h} symmetry, only $^2A_1''$ states will couple with the $^2A_2''$ GS for the Δg_{zz} component. Since the valence s- and p-orbitals of Ga_2As_3 cannot form a_1'' MOs, as was pointed out by Van Zee et al.,[2] DOMO → SOMO and SOMO → virtual MO singly excited $^2A_1''$ states are not possible in the valence region, leading to a small overall value for Δg_{zz}. Although in C_{2v} symmetry the lowest $^2A_2$ state results from a DOMO → SOMO ($1a_2 \rightarrow 3b_1$) excitation, the $1a_2$ MO does not correlate with an a_1'' MO in D_{3h} symmetry, and therefore the $\langle L \rangle$ and $\langle SO \rangle$ matrix elements are extremely small, prohibiting a contribution of 1^2A_2 to Δg_{zz}.

3.3.5. Ga_2As_3 (9). Despite good agreement of experimentally observed with calculated EPR parameters for structure **8** of Ga_2As_3, we calculated these parameters also for structure **9** (C_s symmetry), which is only 0.08 eV higher in energy. This relates to our goal of obtaining properties for all isomers that lie within 0.2 eV of the lowest-energy structure. Table 3 shows that the *g*-tensor components differ widely from those calculated for **8**, and from the experimental values, confirming **8** to be the observed structure. Twenty roots were calculated for **9**, as significant magnetic coupling was observed in the higher $^2A'$ and $^2A''$ states of an initial 9-root calculation.

The largest contributions to the undiagonalized Δg_{xx} arise from coupling of $5^2A''$ and $7^2A''$ with the X^2A' GS. With the exception of $1^2A''$ ($3a''6 \rightarrow a'$, SOMO−1 → SOMO), all other significant couplings (values given in the Supporting Information, Table 5S) with the ground state are negative.

The undiagonalized *yy* component is dominated by the coupling of $5^2A''$ ($8a' \rightarrow 4a''$, SOMO → LUMO+1) with the GS. Coupling from other states making positive and additional negative contributions to Δg_{yy} effectively cancel each other out.

The overall Δg_{zz} is composed mainly of coupling of $2^2A'$ ($3a'' \rightarrow 9a'$, SOMO−1 → LUMO) and $4^2A'$ ($2a'' \rightarrow 8a'$, SOMO−4 → SOMO) with the GS. As with Δg_{yy}, positive and negative contributions from a number of other states cancel each other.

3.3.6. Ga_3As_2 (13). This lowest-energy isomer of Ga_3As_2 has two large Δg components (*x* and *z*), both being in the 100 000 ppm range, and a smaller one (Δg_{yy}) of −15 000 ppm. Twenty roots were calculated for **13** since significant magnetic coupling was observed in the higher $^2A'$ and $^2A''$ states of an initial 9-root calculation.

TABLE 6: Summary of EPR Results for $^{69}Ga_x{}^{75}As_y$ ($x + y = 3, 5$) (all hyperfine coupling constants in MHz)

molecule	atom	A_{iso}	T_{xx}[a]	T_{yy}[a]	T_{zz}[a]	g_{xx}	g_{yy}	g_{zz}	$\langle g \rangle$[b]
$GaAs_2$ (**1**)	Ga	26	−57	131	−74	2.177619	1.827199	1.984039	1.996286
	As	7	−111	−113′	225′				
Ga_2As (**4**)	Ga_1	702	227′	−116′	−112	2.030689	1.991034	1.924319	1.982014
	Ga_2	93	−26′	42′	−16				
	As	−133	312′	−155′	−158				
Ga_2As (**5**)	Ga	447	−63	−81′	144	1.876369	1.977469	2.053349	1.969062
	As	−148	−159	304	−145				
Ga_2As_3 (**8**)	Ga	1325	−65	−65	129	1.928909	1.928909	2.008779	1.955532
	As	−23	−35	−36	71				
Ga_2As_3 (**9**)	Ga_1	9	−32′	70′	−37′	1.938694	1.998779	1.901049	1.946174
	Ga_2	1091	−86′	170	−83′				
	As_1, As_2	−4	58′	−33′	−25′				
	As_3	−69	215′	−112′	−104′				
Ga_2As_3 (expt.)[c]	Ga	1524	−87[d]	−87	174	1.920019	1.920019	2.002319	1.947452
	As	−23	64.7[e]						
Ga_3As_2 (**13**)	Ga_1, Ga_2	125	−23′	−26′	49′	2.137374	1.987249	2.107289	2.077304
	Ga_3	19	−62′	123′	−61				
	As_1	80	−115′	215′	−100				
	As_2	−7	136′	−74′	−62				
Ga_3As_2 (**14**)	Ga_1	1735	−85	−71	156	1.930729	1.990819	2.015589	1.979046
	Ga_2, Ga_3	203	−21	45′	−24′				
	As_1, As_2	−25	−61′	−56	116′				
Ga_3As_2 (**15**)	Ga_1	−3	−28	81	−53	2.182694	2.259979	2.060344	2.167672
	Ga_2, Ga_3	−17	−21′	35	−15′				
	As_1, As_2	87	−106	−109′	215′				
$GaAs_4$ (**18**)	Ga	−153	4	17	−21	1.831289	1.994779	1.987599	1.937889
	As_1, As_2	−46	−156	308′	−152′				
	As_3, As_4	12	−10′	45	−36′				
Ga_4As (**21**)	Ga_1, Ga_2	−122	−89	177′	−88′	1.878779	1.980469	1.958849	1.939366
	Ga_3, Ga_4	153	−34	−43′	76′				
	As	0.05	−13	−7	20				

[a] See footnote *b* in Table 2. [b] Average of the three *g*-tensor components. [c] Ref 2. [d] A_{dip} reported as 87 MHz in ref 2. [e] See footnote *j* in Table 2.

The undiagonalized *xx* component is dominated by the coupling of $1^2A''$ ($3a'' \rightarrow 7a'$, SOMO−1 → SOMO) with the ground state, but other states make large positive and negative contributions to Δg_{xx} (values given in the Supporting Information, Table 6S).

The largest components of Δg_{yy}, $1^2A''$ and $3^2A''$, are relatively small and of opposite sign, with a sum of −16 357 ppm. Although there are a number of other contributing states, the total undiagonalized Δg_{yy} is small (−18 080 ppm) since the positive and negative Δg components from these other excited states nearly cancel each other out.

The Δg_{zz} is dominated by coupling of the GS with $2^2A''$ ($6a' \rightarrow 7a'$, SOMO−3 → SOMO) and $4^2A'$ ($5a' \rightarrow 7a'$, SOMO−4 → SOMO). Large positive contributions from $5^2A'$ and $6^2A'$ are canceled by $3,7,8,9,17^2A'$.

3.3.7. Ga_3As_2 (14). Our calculations show that **14** lies only 0.02 eV above **13**. According to Table 3, these two compounds can be easily distinguished experimentally by their *g*-tensors (and HFCC, discussed above). Although the Δg_{yy} components are similar for **13** and **14**, both Δg_{xx} and Δg_{zz} are much larger for **13** than **14** (see Table 3). Fifteen roots were calculated for **14**, as significant magnetic coupling was observed in the higher $^2B_1$ states of an initial 9-root calculation.

The Δg_{xx} value is governed by the coupling of 1^2B_2 and 3^2B_2 with the X^2A_1 ground state (Table 4), both making large negative contributions to Δg_{xx}.

There are numerous contributions to Δg_{yy}, the largest being 1^2B_1 ($2b_1 \rightarrow 5a_1$, SOMO−3 to SOMO) and 3^2B_1 ($5a_1 \rightarrow 3b_1$, SOMO to LUMO+2), which almost cancel each other. The overall Δg_{yy} is relatively small, with most of the other small negative contributions ($2,4,6,14^2B_1$) being negated by the positive contributions from 5^2B_1 and 11^2B_1 (values given in the Supporting Information, Table 7S).

The overall Δg_{zz} is also small, due to canceling contributions from pairs of states generated by three-open-shell configurations. Contributions to Δg_{zz} from 2^2A_2 and 3^2A_2, both having the same configuration, almost cancel each other: their ΔE values are nearly identical, and although the $\langle SO \rangle$ of 2^2A_2 is ca. 70% larger than that of 3^2A_2, the $\langle L \rangle$ value for 2^2A_2 is ca. 80% smaller than that of 3^2A_2 (and of opposite sign). The leading configuration for 4^2A_2 and 5^2A_2 is the same ($1a_2 \rightarrow 6a_1$, SOMO−2 to LUMO+1), but the respective Δg's differ vastly in magnitude, due to mixing of configurations.

3.3.8. Ga_3As_2 (15). Structure **15** of Ga_3As_2 lies 0.18 eV above the lowest-energy structure **13**, so it is an unlikely competitor for the equilibrium structure. It has two very large components, Δg_{xx} and Δg_{yy}, both being positive, and a smaller but still positive Δg_{zz}. From such *g*-tensors, structure **15** can be easily distinguished from both isomers **13** and **14**. Twenty roots were calculated for **15** since significant magnetic coupling was observed in the higher $^2A_1$, $^2A_2$, and $^2B_1$ states of an initial 9-root calculation.

The Δg_{xx} component is composed mainly of positive couplings of 1^2A_1 ($5a_1 \rightarrow 2b_2$, SOMO−3 → SOMO) and 2^2A_1 ($4a_1 \rightarrow 2b_2$, SOMO−4 → SOMO) with the X^2B_2 GS. Other large positive couplings from $3,4,6,10^2A_1$ are effectively canceled by 5^2A_1 and 12^2A_1.

The Δg_{yy} component is dominated by coupling with 1^2A_2 ($1a_2 \rightarrow 2b_2$, SOMO−2 → SOMO). The net contribution of higher states, making large positive and negative contributions to Δg_{yy}, is only −80 ppm.

Similarly, the Δg_{zz} component is governed by the coupling with 1^2B_1 ($2b_1 \rightarrow 2b_2$, SOMO−1 → SOMO). A number of states contribute positively and negatively to Δg_{zz}, with a net contribution of about −4500 ppm.

*3.3.9. $GaAs_4$ (**18**).* For $GaAs_4$, one very large negative (Δg_{xx}) and two small negative (Δg_{yy}, Δg_{zz}) components were found. The Ga atom lies on the *z*-axis, and As_1-As_2 in the *yz*-plane; As_3 and As_4 lie in the *xz*-plane. Fifteen roots were calculated for **18** since significant magnetic coupling was observed in the higher $^2A_1$, $^2A_2$, and $^2B_1$ states of an initial 9-root calculation.

The Δg_{xx} component is dominated by coupling with 1^2A_1 ($3b_2 \rightarrow 6a_1$, SOMO to LUMO). Large negative contributions from $2,5^2A_1$ are effectively canceled by $4,9^2A_1$.

In contrast to Δg_{xx}, the overall Δg_{yy} and Δg_{zz} values are small due to canceling positive and negative Δg components from numerous excited states. For Δg_{yy}, large contributions from 1^2A_2 and 2^2A_2 are of opposite sign (three open shells) and nearly cancel. The next largest contributions arise from 5^2A_2 and 10^2A_2, both being positive, effectively canceled by negative contributions from a number of states (values given in the Supporting Information, Table 9S).

The largest contributions to Δg_{zz}, from 1^2B_1 and 2^2B_1, are again of opposite sign (one being of DOMO $\rightarrow$ SOMO type, the other SOMO $\rightarrow$ virtual MO). Next largest in magnitude are contributions from 8^2B_1 and 11^2B_1, which have the same three-open-shell configuration. Due to other contributing states, the final Δg_{zz} is again relatively small.

*3.3.10. Ga_4As (**21**).* For this planar C_{2v} structure of Ga_4As, all three Δg components are negative (as was the case for $GaAs_4$), with Δg_{xx} being large, and the other two much smaller. Fifteen roots were calculated for **21**, as significant magnetic coupling was observed in the higher $^2B_1$ and $^2A_2$ states of an initial 9-root calculation.

For Δg_{xx}, the magnetic coupling is dominated by two excited states ($1,2^2B_2$), both having the same two leading configurations ($5a_1 \rightarrow 4b_2$ and $3b_2 \rightarrow 5a_1$) but opposite composition (1^2B_2: 62% and 29%; 2^2B_2: 29% and 63%, respectively). Both states contribute negatively, despite the dominant configuration of 2^2B_2 being of DOMO $\rightarrow$ SOMO type.

The largest contributions to Δg_{yy} are from high-lying excited states ($6,7,8^2B_1$). All of the states contributing significantly to Δg_{yy} had negative Δg components with the exception of 5^2B_1, which is one of a pair of states (with 6^2B_1) from a three-open-shell configuration ($4a_1 \rightarrow 2b_1$).

High-lying states also dominate Δg_{zz}, with the largest negative contributions from $6,7,12,14^2A_2$. The largest positive Δg contribution arises from 11^2A_2, which has the same three-open-shell configuration as 12^2A_2 ($3b_2 \rightarrow 3b_1$), although neither state is dominated by this configuration (42% for 11^2A_2, 60% for 12^2A_2). The other state with a positive contribution to Δg_{zz} is 4^2A_2, which has the same leading three-open-shell configuration as 6^2A_2 ($3b_2 \rightarrow 2b_1$); here the $\langle SO \rangle$ values are quite different and the ΔE's differ by ca. 1 eV. The two Δg contributions are opposite in sign but very dissimilar in magnitude (see Supporting Information, Table 10S).

4. Vertical Excitation Energies

The first five vertical excitation energies for each irreducible representation and the corresponding leading configurations are given in Table 5 for all Ga_xAs_y ($x + y = 3, 5$) isomers within 0.2 eV of the lowest-energy structure. These isomers exhibit a high density of excited states, with all calculated excited states (up to 20 roots) lying within 5.5 eV of the ground state.

No theoretical or experimental vertical excitation energies are found in the literature, but calculated adiabatic values are reported for $GaAs_2$,[11,13,15] Ga_2As,[13] Ga_2As_3, and Ga_3As_2.[18] For Ga_2As_3 and Ga_3As_2, the geometries of the adiabatic excited states reported in ref 18 are significantly different from the ground-state geometry, resulting in poor comparison with our vertical excitation energies. They will not be discussed any further.

For $GaAs_2$, Meier et al. reported an adiabatic excitation energy of 0.65 eV for 1^2A_1,[11] in good agreement with the experimental (photoelectron spectroscopy) value of 0.694 ± 0.077 eV.[42] This is significantly different from our vertical value of 1.47 eV, due to the much shorter Ga−As bond length of 2.49 Å in the adiabatic 1^2A_1 state, compared to the ground state.[11] The adiabatic value of ref 11 is in agreement with Balasubramanian's result for 1^2A_1 of 0.71 eV.[13] The geometry of the 1^2B_1 state reported in ref 13, with a Ga−As bond length of 2.76 Å and an angle of 51.4°, is close to our ground-state geometry (2.775 Å, 46.5°), and the adiabatic energy of 2.08 eV is comparable with our vertical excitation energy of 2.27 eV. The 1^2A_2 state (2.90 Å, 46.5°) from ref 13 lies 1.09 eV above the ground state, close to our vertical excitation energy of 1.26 eV.

For Ga_2As (**5**), Balasubramanian reports adiabatic values of 0.19 and 0.22 eV for 1^2A_1 (Ga−As = 2.47 Å, angle = 118.5°) and 1^2B_1 (2.52 Å, 108.2°),[13] similar to our respective vertical excitation energies of 0.17 and 0.33 eV. For both excited states, the optimized geometry is close to that of the ground state (2.407 Å, 79.9° (ref 13); 2.384 Å, 96.3° (this work)).

5. Summary and Conclusions

The main purpose of this paper was the study of EPR parameters for gallium arsenide clusters up to five atoms. Since not all geometries were known, and some were uncertain, in the first step all geometries were optimized for a number of possible structures.

For $GaAs_2$, the lowest-energy structure has C_{2v} symmetry, in agreement with previous reports.[10−15] For Ga_2As, a C_{2v} and a C_s structure are in competition, with the first one found 0.025 eV below the second one by Balasubramanian,[15] and the opposite ordering, with a 0.02 eV gap, found by us. For Ga_2As_3 we concur with the previous experimental[2] and theoretical[14,16−18] evidence for a D_{3h} structure, although we find a C_s structure to lie only 0.08 eV above the D_{3h} one. For Ga_3As_2, the accepted structure was C_{2v},[14,18] whereas we find a C_s structure, not previously considered, to be 0.02 eV lower in energy. For $GaAs_4$ and Ga_4As, no published geometry parameters could be found. In a paper by Piquini et al. a C_{2v} edge-capped structure was proposed for $GaAs_4$, and a C_{2v} trapezoidal one for Ga_4As (no details of the geometry were given).[19] In comparing them with other possibilities, we confirmed both of them to be the respective lowest-energy structures.

Properties were calculated for all structures lying up to 0.2 eV above the lowest-energy one; HFCC and *g*-tensor results are summarized in Table 6.

With both Ga and As having p-occupations, the SOMO of the cluster molecules is of p-type, and therefore only relatively small A_{iso}'s, proportional to the s-spin density, but large A_{dip}'s, related to the p-density, are expected. Using the atomic values of A_{iso} for 100% s-occupation as a yardstick, a 1% s-occupation, typical for the cluster molecules, gives $A_{iso}(^{69}Ga) = 122$ MHz and $A_{iso}(^{75}As) = 147$ MHz. Similarly, for a typical 30% p-occupation, A_{dip} values of about 136 MHz for ^{69}Ga and 222 MHz for ^{75}As are expected and have been found. Overall, A_{iso} and A_{dip} values are of similar magnitude, corresponding to highly anisotropic EPR spectra.

On the other hand, components of the *g*-shift (deviation from the electronic g_e) are relatively large. Using explicit sum-over-states expansions of second-order perturbation theory, values for the spin−orbit matrix elements on the order of 200−300

cm^{-1} and low-lying excited states of about 1 eV lead to *g*-shifts of about 100 000 ppm, corresponding to changes in the *g*-factor by ±0.1. First-order perturbation contributions have not been calculated and are expected to be relatively small, on the order of several hundred ppm.

From our findings for HFCCs, we confirm the EPR spectral assignment of Ga_2As_3 to correspond to the D_{3h} structure, with the calculated $A_{iso}(^{69}Ga)$ lying about 13% below the experimental value. For the two structures of Ga_2As that are within 0.02 eV of each other, the highest $A_{iso}(^{69}Ga)$ values differ by a factor of 2. On the basis of this and other calculated values, a distinction by EPR should be easy. For Ga_3As_2, also having two structures 0.02 eV apart, the largest $A_{iso}(^{69}Ga)$ is 125 MHz for one and 1735 MHz for the other, again providing sufficient information for determining the correct structure based on EPR spectroscopy. Only one low-energy structure was found for $GaAs_4$ and Ga_4As, so the HFCCs obtained serve as prediction for future EPR studies.

A similar situation applies to the calculated *g*-tensors. Due to sufficiently large differences in the *g*-components, a distinction between the competing structures of Ga_2As should be possible. The calculated *g*-shifts for Ga_2As_3 lie within about 10% of the observed ones, again confirming the experimental assignment of a D_{3h} structure. For the two isomers of Ga_3As_2, close in energy, calculated *g*-shifts differ both in magnitude and sign, allowing for their distinction by EPR spectroscopy.

At this time, the calculation of hyperfine parameters is well established, and in most situations reliable HFCCs can be obtained by using density functional methods. For *g*-tensors, however, density functional methods are still somewhat unreliable, and in many cases poor results are obtained.[35] Also, for different functionals, the results can vary widely. On the other hand, the present study and many previous ones (e.g., refs 25, 27−29, 35) have shown that explicit second-order perturbation state-by-state methods based on MRCI wave functions lead to *g*-shifts usually within 10% of the observed ones. While such calculations are more expensive in terms of computer time, efficiencies in programming and advances in computer hardware allow for applications to larger systems. In future work, the present study of GaAs clusters is to be extended to larger ones, having up to 12 and more atoms. The more daunting prospect here is finding the appropriate geometry, as many more structures are competing for the lowest-energy isomer, with the increasing likelihood of missing some important starting structures.

Acknowledgment. This work was supported by a grant from the U.S. Air Force Office of Scientific Research (AFOSR) in Arlington, VA. We thank Major Daniel K. Johnstone for the award of the grant, and Dr. Shashi Karna for his help, encouragement, and discussions. We are grateful to Prof. Stefan Grimme at the University of Muenster for making his RI-MRCI programs available to us, and to Prof. Christel Marian at the University of Duesseldorf for permission to use the mean-field method for spin−orbit calculations. We also thank Dr. Pablo Bruna for helpful discussions and for reading the manuscript, and Alan Pickard and Andrew MacKay for help with geometry optimizations of the Ga_xAs_y clusters. A contribution from NSERC (Canada) is also acknowledged.

Supporting Information Available: Calculated values of ΔE, $\langle SO \rangle$, $\langle L \rangle$, and Δg (second order) for the first five excited states and those having a large magnetic coupling (>1000 ppm) with the ground state for $GaAs_2$ (**1**), Ga_2As (**4**, **5**), Ga_2As_3 (**8**, **9**), Ga_3As_2 (**13**, **14**, **15**), $GaAs_4$ (**18**), and Ga_4As (**21**) are available free of charge via the Internet at http://pubs.acs.org.

References and Notes

(1) Knight, L. B., Jr.; Hill, D. W.; Kirk, T. J.; Arrington, C. A. *J. Phys. Chem.* **1992**, *96*, 555.
(2) Van Zee, R. J.; Li, S.; Weltner, W., Jr. *J. Chem. Phys.* **1993**, *98*, 4335.
(3) Knight, L. B., Jr.; Petty, J. T. *J. Chem. Phys.* **1988**, *88*, 481.
(4) Knight, L. B., Jr.; Herlong, J. O. *J. Chem. Phys.* **1989**, *91*, 69.
(5) Stein, D.; v. Klitzing, K.; Weimann, G. *Phys. Rev. Lett.* **1983**, *51*, 130.
(6) Kauffmann, U.; Schneider, J.; Räuber, A. *Appl. Phys. Lett.* **1976**, *29*, 312.
(7) Wagner, R. J.; Krebs, K. J.; Strauss, G. H.; White, A. M. *Solid State Commun.* **1980**, *36*, 15.
(8) Kennedy, T. A.; Wilsey, N. D. *Appl. Phys. Lett.* **1984**, *44*, 1089.
(9) Kennedy, T. A.; Wilsey, N. D. *Phys. Rev. Lett.* **1978**, *41*, 977.
(10) Quek, H. K.; Feng, Y. P.; Ong, C. K. *Z. Phys. D* **1997**, *42*, 309.
(11) Meier, U.; Peyerimhoff, S. D.; Grein, F. *Chem. Phys.* **1991**, *150*, 331.
(12) Das, K. K.; Balasubramanian, K. *J. Chem. Phys.* **1991**, *94*, 6620.
(13) Balasubramanian, K. *J. Phys. Chem. A* **2000**, *104*, 1969.
(14) Lou, L.; Nordlander, P.; Smalley, R. E. *J. Chem. Phys.* **1992**, *97*, 1858.
(15) Balasubramanian, K. *J. Chem. Phys.* **1987**, *87*, 3518.
(16) Arratia-Pérez, R.; Hernández-Acevedo, L. *J. Chem. Phys.* **1998**, *109*, 3497.
(17) Lou, L.; Wang, L.; Chibante, L. P. F.; Laaksonen, R. T.; Nordlander, P.; Smalley, R. E. *J. Chem. Phys.* **1991**, *94*, 8015.
(18) Liao, M. Z.; Dai, D.; Balasubramanian, K. *Chem. Phys. Lett.* **1995**, *239*, 124.
(19) Piquini, P.; Canuto, S.; Fazzio, A. *Nanostruct. Mater.* **1998**, *10*, 635.
(20) Piquini, P.; Canuto, S.; Fazzio, A. *Int. J. Quantum Chem. Quantum Chem. Symp.* **1994**, *28*, 571.
(21) Balsubramanian, K.; Zhu, Z. *J. Chem. Phys.* **2001**, *115*, 8858.
(22) (a) Yang, C. Y.; Case D. A. In *Local Density Approximations in Quantum Chemistry and Physics*; Dahl, J. P., Avery, J., Eds.; Plenum: New York, 1983. (b) Arratia-Pérez, R.; Case, D. A. *J. Chem. Phys.* **1983**, *79*, 4939. (c) Arratia-Pérez, R.; Malli, G. L. *J. Chem. Phys.* **1986**, *85*, 6610. (d) Arratia-Pérez, R.; Hernández-Acevedo, L.; Gómez-Jeria, J. S. *Chem. Phys. Lett.* **1995**, *236*, 37. (e) Pablo-Vásquez, J.; Arratia-Pérez, R. *J. Phys. Chem.* **1994**, *98*, 5627. (f) Arratia-Pérez, R.; Hernández-Acevedo, L.; Alvarez-Thon, L. *J. Chem. Phys.* **1998**, *108*, 5795.
(23) Arratia-Pérez, R.; Hernández-Acevedo, L.; Weiss-López, B. *J. Chem. Phys.* **1999**, *110*, 10882.
(24) Frisch, M. J.; Trucks, G. W.; Schlegel, H. B.; Scuseria, G. E.; Robb, M. A.; Cheeseman, J. R.; Zakrzewski, V. G.; Montgomery, J. A., Jr.; Stratmann, R. E.; Burant, J. C.; Dapprich, S.; Millam, J. M.; Daniels, A. D.; Kudin, K. N.; Strain, M. C.; Farkas, O.; Tomasi, J.; Barone, V.; Cossi, M.; Cammi, R.; Mennucci, B.; Pomelli, C.; Adamo, C.; Clifford, S.; Ochterski, J.; Petersson, G. A.; Ayala, P. Y.; Cui, Q.; Morokuma, K.; Malick, D. K.; Rabuck, A. D.; Raghavachari, K.; Foresman, J. B.; Cioslowski, J.; Ortiz, J. V.; Stefanov, B. B.; Liu, G.; Liashenko, A.; Piskorz, P.; Komaromi, I.; Gomperts, R.; Martin, R. L.; Fox, D. J.; Keith, T.; Al-Laham, M. A.; Peng, C. Y.; Nanayakkara, A.; Gonzalez, C.; Challacombe, M.; Gill, P. M. W.; Johnson, B. G.; Chen, W.; Wong, M. W.; Andres, J. L.; Head-Gordon, M.; Replogle, E. S.; Pople, J. A. *Gaussian 98*, revision A.9; Gaussian, Inc.: Pittsburgh, PA, 1998.
(25) (a) Lushington, G. H.; Grein, F. *J. Chem. Phys.* **1995**, *106*, 3292. (b) Lushington, G. H.; Bündgen, P.; Grein, F. *Int. J. Quantum Chem.* **1995**, *55*, 377. (c) Lushington, G. H.; Grein, F. *Theor. Chim. Acta* **1996**, *93*, 259. (d) Lushington, G. H.; Grein, F. *Int. J. Quantum Chem.* **1996**, *60*, 1679. (e) Lushington, G. H. Ph.D. Thesis, University of New Brunswick, Fredericton, NB, Canada, 1996.
(26) Weltner. W., Jr. *Magnetic Atoms and Molecules*; Dover: New York, 1983.
(27) Bruna, P. J.; Lushington, G. H.; Grein, F. *J. Mol. Struct.* **2000**, *527*, 139, and references therein.
(28) Bruna, P. J.; Grein, F. *J. Chem. Phys.* **2000**, *112*, 10796, and references therein.
(29) Bruna, P. J.; Grein, F. *Chem. Phys.* **2002**, *276*, 1.
(30) Ahlrichs, R.; Bär, M.; Häser, M.; Horn, H.; Kölmel, C. *Chem. Phys. Lett.* **1989**, *162*, 165.
(31) (a) Grimme, S.; Waletzke, M. *J. Chem. Phys.* **1999**, *111*, 5645. (b) Grimme, S.; Waletzke, M. *Phys. Chem. Chem. Phys.* **2000**, *2*, 2075.

(32) Hess, B. A.; Marian, C. M.; Wahlgren, U.; Gropen, O. *Chem. Phys. Lett.* **1996**, *251*, 365.

(33) Schimmelpfennig, B. *Atomic Spin−Orbit Mean-Field Integral Program*; Stockholms Universitet: Sweden, 1996.

(34) Kleinschmidt, M.; Tatchen, J.; Marian, C. M. *J. Comput. Chem.* **2002**, *23*, 824.

(35) Brownridge, S.; Grein, F.; Tatchen, J.; Kleinschmidt, M.; Marian, C. M. *J. Chem. Phys.* **2003**, *118*, 9552.

(36) Schäfer, A.; Huber, C.; Ahlrichs, R. *J. Chem. Phys.* **1994**, *100*, 5829.

(37) Luzanov, A. V.; Babich, E. N.; Ivanov, V. V. *J. Mol. Struct. (THEOCHEM)* **1994**, *331*, 211.

(38) (a) Vasiliev, I.; Öğüt, S.; Chelikowsky, J. R. *Phys. Rev. Lett.* **1997**, *78*, 4085. (b) Vasiliev, I.; Öğüt, S.; Chelikowsky, J. R. *Phys. Rev. B* **1999**, *60*, R8477.

(39) Lefebvre-Brion, H.; Field, R. W. *Perturbations in the Spectra of Diatomic Molecules*; Academic Press: Orlando, FL, 1986; Table 4.6, p 214.

(40) Lushington, G. H.; Grein, F. *J. Chem. Phys.* **1997**, *106*, 3292.

(41) Törring, J. T.; Un, S.; Knüpling, M.; Plato, M.; Möbius, K. *J. Chem. Phys.* **1997**, *107*, 3905.

(42) Taylor, T. R.; Gomez, H.; Asmis, K. R.; Neumark, D. M. *J. Chem. Phys.* **2001**, *115*, 4620.